Journal of Power Sources 223 (2013) 336–340

Contents lists available at SciVerse ScienceDirect

Journal of Power Sources

journal homepage: www.elsevier.com/locate/jpowsour

Short communication

Ion beam-mixed Ge electrodes for high capacity Li rechargeable batteries

N.G. Rudawski [a,*], B.R. Yates [a], M.R. Holzworth [a], K.S. Jones [a], R.G. Elliman [b], A.A. Volinsky [c]

[a] Department of Materials Science and Engineering, University of Florida, 100 Rhines Hall, PO Box 116400, Gainesville, FL 32611-6400, USA
[b] Department of Electronic Materials Engineering, Research School of Physics and Engineering, Australian National University, Canberra, Australian Capital Territory 0200, Australia
[c] Department of Mechanical Engineering, University of South Florida, Tampa, FL 33620, USA

HIGHLIGHTS

- The electrochemical performance of ion beam-mixed Ge film electrodes was studied.
- Ion beam mixing was effected without altering electrode morphology.
- Ion beam mixing enhanced the adhesion of the electrode to the current collector.
- Ion beam-mixed electrodes exhibited stable specific capacities of ~1500 mAh g^{-1}.
- Electron microscopy was used to study the morphological evolution of electrodes.

ARTICLE INFO

Article history:
Received 13 July 2012
Received in revised form
14 September 2012
Accepted 15 September 2012
Available online 28 September 2012

Keywords:
Ion beam mixing
Ion implantation
Ion beam modification
Ge
Germanium
Li ion battery anode

ABSTRACT

Ion beam modification to effect ion beam mixing without changing morphology was investigated as a means to improve the electrochemical performance of Ge thin film electrodes for rechargeable Li batteries. As a result of a minimum tenfold increase in the strength of adhesion of the Ge film to the current collector (substrate), the ion beam-mixed electrodes exhibited stable specific capacities of ~1500 mAh g^{-1} (close to the theoretical maximum of 1623 mAh g^{-1}) for galvanostatic cycling rates of 0.2C–1.6C using both single- and multi-rate testing schemes. Electron microscopy investigations showed that the ion beam-mixed electrodes transform from a flat, continuous, nonporous microstructure in the virgin state to a rough, cracked, porous microstructure as a result of electrochemical cycling, but remain in excellent electrical contact with the current collector. The results suggest that ion beam mixing could be used to produce inexpensive, high capacity conversion electrodes for rechargeable Li batteries.

1. Introduction

There is great interest in the use of conversion (or synthesizing) electrodes like Si, Ge, and Sn for Li ion battery anodes, which have very large specific capacities 3–11 times that of the traditional graphite intercalation anode [1–3]. However, conversion electrodes experience very large volumetric changes on the order of 300–400% as a result of lithiation (charging) and delithiation (discharging). In film electrodes, this can result in material losing electrical contact due to intra-material fracture and/or delamination at the electrode/current collector interface with a concomitant decrease in electrode capacity with prolonged electrochemical cycling [4]. Typically, addressing the challenge of accommodating the large volumetric changes that occur during cycling of conversion electrodes without material decrepitation has centered on altering the morphology of the electrode [5]. Specifically, it has been shown that conversion electrodes with nanoscale features are able to facilitate stress relaxation during electrochemical cycling without intra-material fracture [6–11]. However, this approach has limitations in terms of practical applicability due to cost, difficulty of fabrication, and total electrode capacity. Furthermore, the approach of altering electrode morphology does not directly address the other major decrepitation mechanism associated with the integrity of the interface between the electrode and current collector.

In principle, the ability of a film electrode to maintain electrical contact with the current collector during electrochemical cycling is directly related to the adhesion strength (also known as work of

* Corresponding author. Tel.: +1 805 252 4916; fax: +1 352 392 7219.
E-mail address: ngr@ufl.edu (N.G. Rudawski).

0378-7753/$ – see front matter © 2012 Elsevier B.V. All rights reserved.
http://dx.doi.org/10.1016/j.jpowsour.2012.09.056

adhesion) between the film and substrate [12–14]. Therefore, all other factors being equal, an electrode with greater adhesion strength should be more resistant to cycling-induced decrepitation and should therefore exhibit superior performance. One well-known method to enhance the adhesion strength of a film to a substrate is by ion beam modification [15–17]. Specifically, it has been shown that ion beam mixing, or atomic-level intermixing between the film and substrate by energetic ion bombardment, can enhance adhesion strength by up to two orders of magnitude [15,18,19]. Recently, it was shown that ion beam modification of Ge film electrodes resulted in a dramatic improvement in electrochemical performance compared to as-prepared electrodes and it was speculated that ion beam mixing might have been a contributing factor [20]. However, it was not possible to isolate the exact role of ion beam mixing on electrochemical performance since the room-temperature ion beam modification step also effected a dramatic change in the morphology of the electrode, which is well known for ion-implanted Ge [21–28]. In this work, it is shown for the first time that ion beam mixing of a conversion electrode/current collector interface results in a significant improvement in the electrochemical performance of the electrode. This improvement is the result of increased adhesion of the Ge film to the current collector and not any change in film morphology.

2. Experimental

Ge electrodes were produced by depositing a 140 nm-thick Ge film onto a $\sim 10 \times 10$ cm^2 area of McMaster-Carr 0.005 cm-thick 80 at.% Ni – 20 at.% foil substrate using room-temperature electron beam evaporation at a rate of 0.5 nm s^{-1} using an *n*-type Ge target with dopant concentration of 1.0×10^{17} cm^{-3}. A portion of this "as-deposited" electrode material was then subjected to ion beam modification at a temperature of 77 K using Ge^+ implantation at an energy of 260 keV and dose of 1.0×10^{16} cm^{-2} to produce "ion beam-modified" electrodes and to effect ion beam mixing of the Ge/substrate interface without altering the morphology of the Ge film [28]. The adhesion strength of the films was studied by performing nanoindentation using a Hysitron Triboindenter equipped with a cube corner tip and by performing scotch tape [29] testing.

Cells for electrochemical testing were prepared in sealed pouches in an Ar atmosphere (H_2O concentration < 0.9 ppm) using 50 μm-thick polypropylene separators and 1.0 M $LiPF_6$ in 1:1 (by volume) ethylene carbonate:dimethyl carbonate (DMC) liquid electrolyte [30] with the Ge film on the Ni–Fe foil as one electrode and Li metal foil as the other electrode (half-cell configuration). The electrochemical properties of the electrodes were evaluated with galvanostatic (constant current) cycling and cyclic voltammetry (voltage sweep rate of 1 mV s^{-1}) using an Arbin BT2000 battery tester. The voltage range for both types of cycling was 0.01–1.50 V as used in other Ge studies [7,31–35]. In the case of galvanostatic cycling, the charge/discharge currents needed to generate the specified cycling rates for each sample were calculated by estimating the Ge mass of each sample using the reported density [36] of evaporated Ge (4.82 g cm^{-3}), the surface area of the electrode, and the 140 nm thickness of the as-deposited films; the typical surface area for an electrode used in this work was $\sim 5 \times 5$ mm^2 with typical charge and discharge currents ranging from 5 to 30 μA (depending on the cycling rate). The estimated experimental error in all mass calculations was ±5%, which results in a corresponding experimental error of the same magnitude for all reported specific capacities. Additionally, loss of Ge mass due to sputtering as a result of ion beam modification is expected to be negligible (<1%) as per simulations [37]; the additional Ge mass resulting from ion beam modification is also negligible (<0.001%). The morphological and structural evolution of the electrodes was evaluated ex-situ with high-resolution cross-sectional transmission electron microscopy (HR-XTEM) using a JEOL 2010F transmission electron microscope and top-down scanning electron microscopy (SEM) using an FEI DB235 dual beam scanning electron microscope/focused ion beam (FIB) system; FIB milling was used to prepare HR-XTEM samples. Prior to FIB processing, samples were coated with a protective C layer while protective Pt layers were deposited in-situ during FIB processing to prevent surface damage. Prior to analyzing cycled electrodes, the cells were reintroduced into the Ar environment used for fabrication and the electrodes given a 1 min wash with DMC to remove remnant electrolyte [38]. Care was taken to minimize exposure of cycled electrodes to air prior to HR-XTEM or SEM analysis.

3. Results and discussion

Fig. 1(a) and (b) present HR-XTEM images comparing the morphology of virgin as-deposited and ion beam-mixed Ge electrodes, respectively. The Ge electrodes are ~140 nm-thick with no detectable difference in film morphology evident between as-deposited and ion beam-modified electrodes, consistent with prior reports of ion beam modification of Ge under similar conditions used in this work [28]. The virgin as-deposited and ion beam-mixed electrodes were also amorphous, as confirmed using selected area electron diffraction (not presented). The distribution

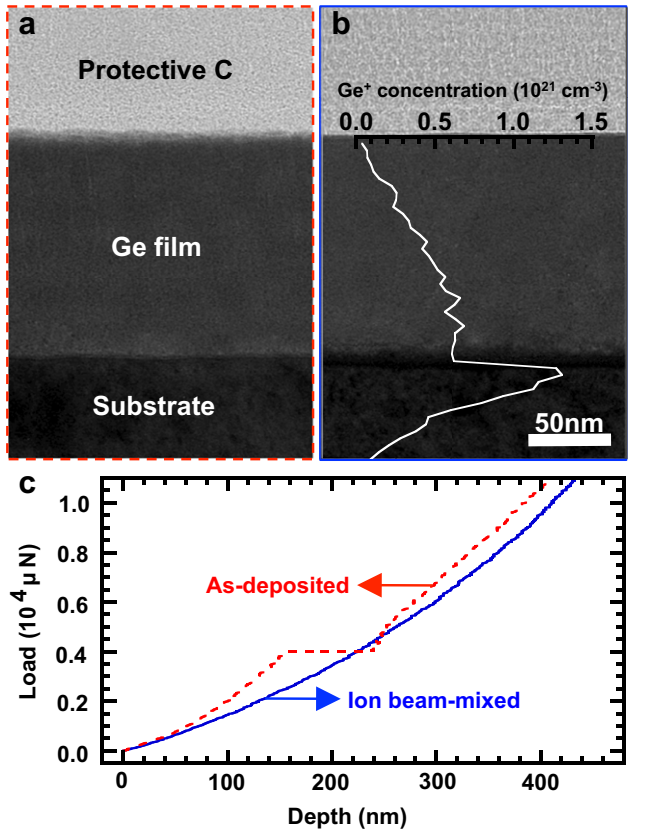

Fig. 1. HR-XTEM images showing the effect of ion beam modification on the morphology of deposited Ge electrodes: a) As-deposited and b) ion beam-modified using Ge^+-implantation at $T = 77$ K with energy of 260 keV and dose of 1.0×10^{16} cm^{-2}. Also shown is the implanted Ge^+ distribution calculated using the Monte Carlo SRIM-code [37]. c) Load versus depth curves for virgin as-deposited and ion beam-mixed Ge electrodes subjected to nanoindentation testing. The as-deposited electrode exhibits a distinct excursion in the load curve at an indentation depth of ~150 nm while the ion beam-mixed electrode exhibits no such excursion, indicating the ion beam-mixed electrode has enhanced strength of adhesion.

of implanted Ge^+ was calculated using the SRIM-Monte Carlo code [37] and is superimposed on Fig. 1(b). This code also predicts ~5 nm of intermixing at the electrode/current collector interface as a result of ion beam modification (Supplementary data). Nanoindentation was used to investigate the effect of ion beam modification on electrode adhesion strength as shown in the load versus depth curves presented in Fig. 1(c). In the case of the as-deposited electrode, there is a distinct discontinuity in the loading curve at an indentation depth of ~150 nm (close to the measured film thickness), which is consistent with delamination of the film from the substrate [39]. Comparatively, the ion beam-mixed electrode did not exhibit any such excursions, indicating no delamination during nanoindentation and confirming the adhesion strength of the ion beam-mixed electrode to be significantly higher than that of the as-deposited counterpart. The enhanced adhesion strength of the ion beam-mixed electrodes was also confirmed using scotch tape testing [29], which resulted in complete delamination of the as-deposited film while the ion beam-mixed film did not delaminate. Based on the results from nanoindentation and scotch tape testing in conjunction with prior work using these methods to quantify film adhesion [29,39], reasonable limits on the adhesion strength of as-deposited and ion beam-mixed electrodes are estimated at <1 and >10 J m^{-2}, respectively, indicating a minimum tenfold increase in adhesion strength due to ion beam modification.

Fig. 2(a) shows the voltage curves for cycles 1, 2, and 25 of an ion beam-mixed Ge electrode subjected to galvanostatic cycling at a 0.4C rate (2.5 h per charge or discharge). The specific charge (discharge) capacity for cycle 1 was 1730 (1527) mAh g^{-1} indicating a Coulombic efficiency of ~88.3% and suggesting the formation of a solid-electrolyte interphase layer [40]. For the subsequent second cycle, the specific charge (discharge) capacity was 1547 (1515) mAh g^{-1} with a coulombic efficiency of ~97.9%. The voltage curve for cycle 25 was nearly identical to that of cycle 2, with a specific charge (discharge) capacity of 1540 (1486) mAh g^{-1} and a coulombic efficiency of ~96.5% suggesting virtually no capacity fade over 25 cycles. All three voltage curves share similar features, most notably the distinct plateau at ~0.50 V during delithiation, which are consistent with reported voltage curves for the electrochemical cycling Ge with Li [7,31–35]. Additionally, ion beam-mixed electrodes cycled at 0.2C, 0.8C, and 1.6C rates for 25 cycles exhibited basically identical voltage curves for cycles 1, 2, and 25 compared to the case of cycling at a 0.4C rate (Supplementary data). Fig. 2(b) presents cyclic voltammograms for cycles 1 and 64 of an ion beam-mixed Ge film collected with a voltage sweep rate of 1 mV s^{-1}. During cycle 1, there were distinct cathodic peaks at voltages of ~0.41, 0.27, and ~0.028 V with a single distinct anodic peak at ~0.69 V. After 64 cycles, a single distinct cathodic peak was evident at a voltage of ~0.082 while two distinct anodic peaks were observed at voltages of ~0.44 and ~0.55 V. The shifting in the voltages at which peaks were observed is consistent with prior reports of cyclic voltammetry of conversion electrode materials and has been attributed to cycling-induced changes in electrode morphology [6]. Similarly to the voltage curves, the reported cyclic voltammetry data is consistent with previous reports of electrochemical cycling of Ge with Li [31].

Fig. 2(c) presents cycle life behavior for as-deposited and ion beam-mixed Ge electrodes cycled at a 0.4C rate. The specific capacity of the as-deposited electrode faded very rapidly with cycling with specific charge and discharge capacities of ~75 mAh g^{-1} after 25 cycles, which indicates the loss of electrical contact of active material as a result of cycling. In contrast, the ion beam-mixed electrode exhibited virtually no capacity fade over 25 cycles with stable specific charge and discharge capacities of ~1500 mAh g^{-1} and coulombic efficiencies greater than 96.5%. This indicates no loss of electrical contact of active material with cycling and shows a remarkable ~2000% improvement in performance compared to the as-deposited electrode. Additionally, ion beam-mixed electrodes were also cycled at 0.2C, 0.8C, and 1.6C rates for

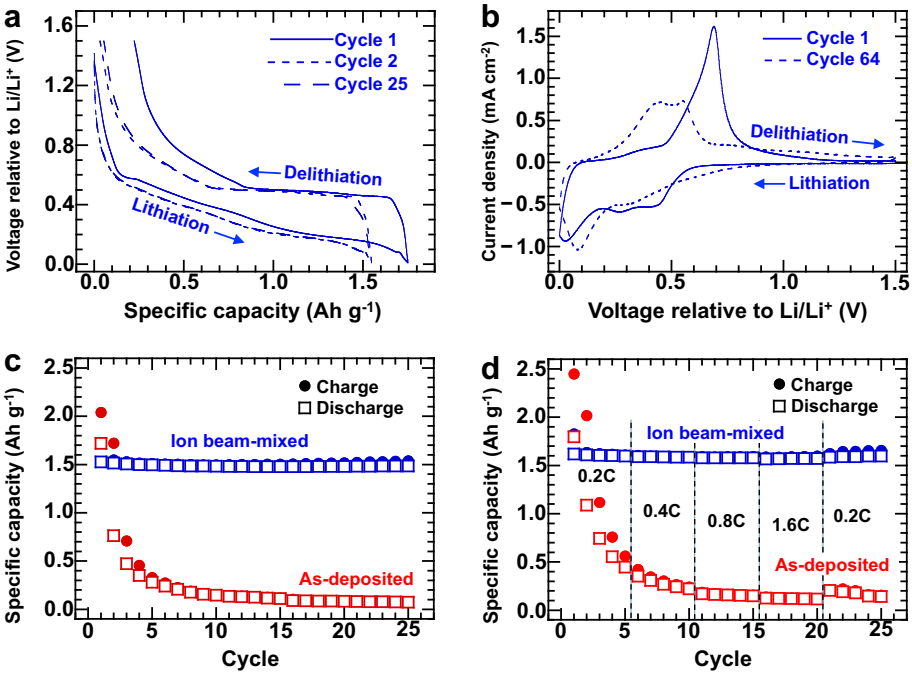

Fig. 2. Electrochemical cycling data for Ge electrodes: a) Voltage curves for cycles 1, 2, and 25 of an ion beam-mixed electrode galvanostatically cycled at a 0.4C rate, b) cyclic voltammograms (sweep rate of 1 mV s^{-1}) for cycles 1 and 64 of an ion beam-mixed electrode, c) cycle life plot for as-deposited and ion beam-mixed electrodes galvanostatically cycled at a 0.4C rate for 25 cycles, and d) cycle life plot for as-deposited and ion beam-mixed electrodes galvanostatically cycled sequentially at 0.2C, 0.4C, 0.8C, 1.6C, and 0.2C for 5 cycles each (25 cycles total).

25 cycles and exhibited virtually no capacity fade over 25 cycles with stable specific charge and discharge capacities of ~1500 mAh g^{-1}, very similar to the case of cycling at a 0.4C rate shown in Fig. 2(c) (Supplementary data). Additionally, as-deposited and ion beam-mixed electrodes were also subjected to galvanostatic cycling at a 1.6C rate for 200 cycles (Supplementary data). The specific charge and discharge capacities of the as-deposited electrode faded rapidly to ~60 mAh g^{-1} after 200 cycles. In comparison, the ion beam-mixed electrode exhibited capacity fading, but the specific charge and discharge capacities were still ~650 mAh g^{-1}, which is an improvement of ~900% compared to the as-deposited electrode.

Fig. 2(d) shows the cycle life performance of as-deposited and ion beam-mixed electrodes subjected to galvanostatic cycling sequentially at 0.2C, 0.4C, 0.8C, 1.6C, and 0.2C for 5 cycles each (25 cycles total). The as-deposited electrode showed dramatic capacity fading with specific charge and discharge capacities of ~120 mAh g^{-1} observed at a 1.6C rate; upon returning the cycling rate to 0.2C, specific charge and discharge capacities of only ~150 mAh g^{-1} were retained, which again indicates the loss of electrical contact of active material. The ion beam-mixed electrode subjected to the same cycling scheme showed virtually no capacity fade even at a cycling rate of 1.6C with stable specific charge and discharge capacities >1500 mAh g^{-1}. Upon returning the cycling rate to 0.2C, the specific charge and discharge capacities remained stable and >1500 mAh g^{-1}, which indicates no loss of electrical contact of active material as a result of cycling. The lack of capacity fading with increasing cycling rate using multi-rate and single-rate cycling schemes is particularly noteworthy, since other types of Ge electrodes subjected to similar cycling schemes exhibited pronounced decreases in specific capacity with increasing cycling rate [7,33,41]. Moreover, the electrochemical performance of the ion beam-mixed Ge electrodes is among the best reported for any type of Ge electrode. In particular, the performance is superior to many nanoscale forms of Ge electrodes including nanoparticle composites [8,34], nanowires [7,10], and nanotubes [41,42].

SEM and HR-XTEM were used to investigate the microstructure of ion beam-mixed Ge electrodes subjected to galvanostatic cycling at a 0.4C rate as shown in Fig. 3. Fig. 3(a) and (e) are images of an as-irradiated electrode, showing that it initially exhibits a basically featureless surface and uniform thickness. After 1 cycle, the surface exhibits through-film cracking, as shown in Fig. 3(b), but the electrode remains relatively flat, with ~200 nm peak-to-valley roughening in the vicinity of cracks, as shown in Fig. 3(f). With further cycling to 12 cycles, the crack density increases, as shown in the Fig. 3(c), and the morphology of the electrode transforms into three-dimensional islands with ~300 nm peak-to-valley roughening, as shown in Fig. 3(g). After 25 cycles there is no further change in crack density but the peak-to-valley roughening increases to ~750 nm and the three-dimensional islands extend further above and below the original surface plane, as shown in Fig. 3(h). High-magnification HR-XTEM was also performed on the ion beam-mixed Ge electrodes to study the nanoscale morphological evolution during cycling, as shown in Fig. 4. The virgin electrode was found to be bulk-like with little evidence for porosity, as shown in Fig. 4(a). However, an electrode subjected to galvanostatic cycling at a 0.4C rate for 25 cycles, was found to be highly porous, with pores ~5 nm in diameter evident throughout the material, as shown in Fig. 4(b).

The through-film crack evolution observed for the ion beam-mixed Ge electrodes is very similar to crack evolution reported in other types of thin film conversion electrodes [12,13]. However, the dramatic structural evolution from a continuous flat film to a three-dimensional porous microstructure has not been observed for other thin film conversion electrodes. It is interesting to note, however, that NW forms of conversion electrodes have been shown to develop porosity upon electrochemical cycling [43]; a change attributed to long-range rearrangement and transport of atoms in the material during the insertion and removal of Li (characteristic of conversion electrodes). It has also been shown that the porosity of the NWs increases with the number of electrochemical cycles [43], which is very similar to the morphological evolution observed for the ion beam-mixed Ge electrodes presented in Figs. 3 and 4. In the case of NW electrodes, the small diameters [4] allow the NWs to survive a large number of electrochemical cycles without decrepitation [6,7,44], which explains the observation of increasing porosity with prolonged electrochemical cycling (i.e. premature failure of the electrodes precludes the observation of such structural evolution). Similar arguments can be used to explain the structural evolution of ion beam-mixed Ge electrodes.

As a result of this morphological evolution, the ion beam-mixed electrodes acquire a very high surface area to volume ratio, which

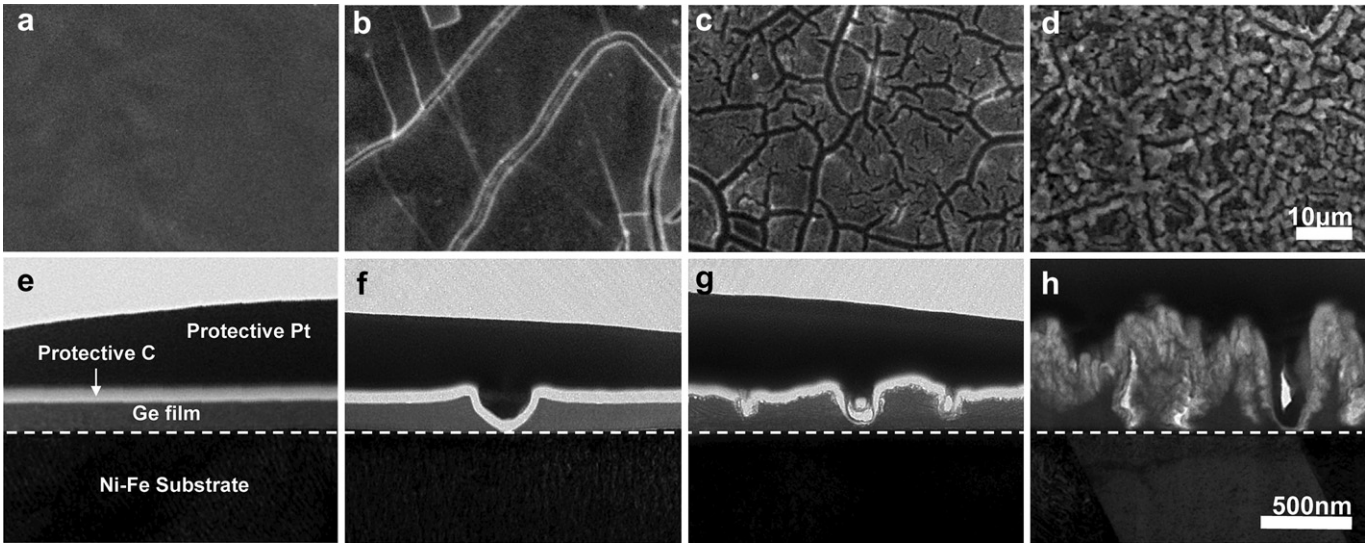

Fig. 3. The morphological evolution of ion beam-mixed Ge electrodes galvanostatically cycled at a 0.4C rate. Top-down SEM images of electrodes after (a) 0, (b) 1, (c) 12, and (d) 25 cycles. HR-XTEM images of electrodes after (e) 0, (f) 1, (g) 12, and (h) 25 cycles; the protective C/Pt layers, Ge film, and Ni–Fe foil substrate are indicated.

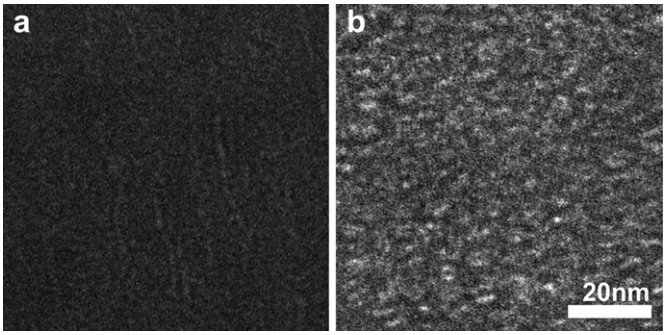

Fig. 4. High-magnification HR-XTEM images showing the generation of a porous microstructure in ion beam-mixed Ge electrodes due to electrochemical cycling: a) virgin electrode and b) an electrode galvanostatically cycled at 0.4C rate for 25 cycles. Both images were taken with defocus $\Delta f \sim -1000$ nm to highlight the presence of any pores.

should facilitate faster Li insertion and extraction during cycling [5]. This explains why there is virtually no fade in the specific capacity of the ion beam-mixed electrodes over 25 cycles for a range of cycling rates as shown in Figs. 3 and 4, which has not been reported for other types of Ge film electrodes. Finally, it should be noted that while only the case of Ge film electrodes with a single thickness was investigated here, the ion beam mixing approach to improving electrode adhesion strength can, in principle, be applied to other types of conversion electrodes of any arbitrary thickness via adjustment of the ion beam modification conditions. The implications of this are significant as this approach could potentially allow for the production of inexpensive, relatively thick Si film electrodes that can be cycled for a large number of cycles without decrepitation. Additionally, this work only investigated one specific ion beam modification condition and the adhesion strength of the electrode should scale with the ion dose assuming the same ion energy [15,18,19]. Therefore, if the electrochemical performance of the electrode scales with the adhesion strength, there should be a distinct relationship between ion dose (at a given ion energy) and electrochemical performance. Experiments are in progress to investigate this.

4. Summary and conclusions

In conclusion, it was shown for the first time that ion beam mixing enhances the strength of adhesion of Ge film electrodes to the current collector and results is in a dramatic improvement in electrochemical performance. Specifically, the ion beam-mixed film electrodes exhibit stable specific capacities close to the theoretical value of Ge for a range of cycling rates and are superior to many nanoscale forms of Ge electrodes. Moreover, this approach of using ion beam modification as a means to improve Ge film electrode performance is very simple, can be readily applied to other types of conversion electrodes, and offers the potential of fabricating high capacity Li ion battery electrodes inexpensively.

Acknowledgments

The authors acknowledge the Major Analytical Instrumentation Center at the University of Florida for use of the transmission electron microscope, scanning electron microscope, and focused ion beam facilities. Microfabritech at the University of Florida is acknowledged for use of the electron beam evaporation system. The Australian Government NCRIS and EIF programs for access to Heavy Ion Accelerator Facilities at the Australian National University are also acknowledged.

Appendix A. Supplementary data

Supplementary data related to this article can be found at http://dx.doi.org/10.1016/j.jpowsour.2012.09.056.

References

[1] H. Okamoto, J. Phase Equilib. Diff. 30 (2009) 118–119.
[2] J. Sangster, C. Bale, J. Phase Equilib. 19 (1998) 70–75.
[3] J. Sangster, A. Pelton, J. Phase Equilib. 18 (1997) 289–294.
[4] R. Huggins, W. Nix, Ionics 6 (2000) 57–63.
[5] P.G. Bruce, B. Scrosati, J.M. Tarascon, Angew. Chem. Int. Ed. 47 (2008) 2930–2946.
[6] C.K. Chan, H.L. Peng, G. Liu, K. McIlwrath, X.F. Zhang, R.A. Huggins, Y. Cui, Nat. Nanotech. 3 (2008) 31–35.
[7] C.K. Chan, X.F. Zhang, Y. Cui, Nano Lett. 8 (2008) 307–309.
[8] M.-H. Park, K. Kim, J. Kim, J. Cho, Adv. Mater. 22 (2010) 415–418.
[9] K.Q. Peng, J.S. Jie, W.J. Zhang, S.T. Lee, Appl. Phys. Lett. 93 (2008) 033105.
[10] M.H. Seo, M. Park, K.T. Lee, K. Kim, J. Kim, J. Cho, Energy Environ. Sci. 4 (2011) 425–428.
[11] J. Yang, M. Winter, J.O. Besenhard, Solid State Ionics 90 (1996) 281–287.
[12] J.C. Li, A.K. Dozier, Y.C. Li, F.Q. Yang, Y.T. Cheng, J. Electrochem. Soc. 158 (2011) A689–A694.
[13] J.P. Maranchi, A.F. Hepp, A.G. Evans, N.T. Nuhfer, P.N. Kumta, J. Electrochem. Soc. 153 (2006) A1246–A1253.
[14] F.Q. Yang, J. Power Sources 196 (2011) 465–469.
[15] J.E.E. Baglin, Nucl. Instrum. Methods Phys. Res. B 65 (1992) 119–128.
[16] J.E.E. Baglin, IBM J. Res. Dev. 38 (1994) 413–422.
[17] J.E.E. Baglin, G.J. Clark, Nucl. Instrum. Methods Phys. Res. B 7-8 (1985) 881–885.
[18] K.H. Chae, J.H. Joo, I.S. Choi, K.S. Kim, S.S. Kim, C.N. Whang, H.K. Kim, D.W. Moon, J. Korean Phys. Soc. 26 (1993) 612–616.
[19] L. Guzman, A. Miotello, R. Checchetto, M. Adami, Surf. Coat. Technol. 158 (2002) 558–562.
[20] N.G. Rudawski, B.L. Darby, B.R. Yates, K.S. Jones, R.G. Elliman, A.A. Volinsky, Appl. Phys. Lett. 100 (2012) 083111.
[21] B.R. Appleton, O.W. Holland, D.B. Poker, J. Narayan, D. Fathy, Nucl. Instrum. Methods Phys. Res. B 7–8 (1985) 639–644.
[22] B.L. Darby, B.R. Yates, N.G. Rudawski, K.S. Jones, A. Kontos, R.G. Elliman, Thin Solid Films 519 (2011) 5962–5965.
[23] O.W. Holland, B.R. Appleton, J. Narayan, J. Appl. Phys. 54 (1983) 2295–2301.
[24] H. Huber, W. Assmann, S.A. Karamian, A. Mucklich, W. Prusseit, E. Gazis, R. Grotzschel, M. Kokkoris, E. Kossionidis, H.D. Mieskes, R. Vlastou, Nucl. Instrum. Methods Phys. Res. B 122 (1997) 542–546.
[25] R.J. Kaiser, S. Koffel, P. Pichler, A.J. Bauer, B. Amon, A. Claverie, G. Benassayag, P. Scheiblin, L. Frey, H. Ryssel, Thin Solid Films 518 (2010) 2323–2325.
[26] E.M. Lawson, K.T. Short, J.S. Williams, B.R. Appleton, O.W. Holland, O.E. Schow, Nucl. Instrum. Methods Phys. Res. 209 (1983) 303–307.
[27] L. Romano, G. Impellizzeri, M.V. Tomasello, F. Giannazzo, C. Spinella, M.G. Grimaldi, J. Appl. Phys. 107 (2010) 084314.
[28] B. Stritzker, R.G. Elliman, J. Zou, Nucl. Instrum. Methods Phys. Res. B 175 (2001) 193–196.
[29] P.A. Steinmann, H.E. Hintermann, J. Vac. Sci. Technol. A 7 (1989) 2267–2272.
[30] K. Xu, Chem. Rev. 104 (2004) 4303–4417.
[31] L. Baggetto, P.H.L. Notten, J. Electrochem. Soc. 156 (2009) A169–A175.
[32] J. Graetz, C.C. Ahn, R. Yazami, B. Fultz, J. Electrochem. Soc. 151 (2004) A698–A702.
[33] B. Laforge, L. Levan-Jodin, R. Salot, A. Billard, J. Electrochem. Soc. 155 (2008) A181–A188.
[34] H. Lee, H. Kim, S.G. Doo, J. Cho, J. Electrochem. Soc. 154 (2007) A343–A346.
[35] L.C. Yang, Q.S. Gao, L. Li, Y. Tang, Y.P. Wu, Electrochem. Commun. 12 (2010) 418–421.
[36] G. Peto, Z.F. Horvath, O. Gereben, L. Pusztai, F. Hajdu, E. Svab, Phys. Rev. B 50 (1994) 539–542.
[37] J.F. Ziegler, Nucl. Instrum. Methods Phys. Res. B 219 (2004) 1027–1036.
[38] G.M. Veith, N.J. Dudney, J. Electrochem. Soc. 158 (2011) A658–A663.
[39] A.A. Volinsky, N.R. Moody, W.W. Gerberich, Acta Mater. 50 (2002) 441–466.
[40] E. Peled, J. Electrochem. Soc. 126 (1979) 2047–2051.
[41] G.L. Cui, L. Gu, N. Kaskhedikar, P.A. van Aken, J. Maier, Electrochim. Acta 55 (2010) 985–988.
[42] R.A. DiLeo, M.J. Ganter, R.P. Raffaelle, B.J. Landi, J. Mater. Res. 25 (2010) 1441–1446.
[43] J.W. Choi, J. McDonough, S. Jeong, J.S. Yoo, C.K. Chan, Y. Cui, Nano Lett. 10 (2010) 1409–1413.
[44] K. Kang, H.S. Lee, D.W. Han, G.S. Kim, D. Lee, G. Lee, Y.M. Kang, M.H. Jo, Appl. Phys. Lett. 96 (2010) 053110.